

## Metabolic syndrome and adiposity: Risk factors for decreased myelin in cognitively healthy adults

Agnieszka Z Burzynska<sup>a,\*</sup>, Charles Anderson<sup>b</sup>, David B Arciniegas<sup>c,d</sup>, Vince Calhoun<sup>e</sup>, In-Young Choi<sup>f</sup>, Andrea Mendez Colmenares<sup>a</sup>, Grace Hiner<sup>a</sup>, Arthur F Kramer<sup>g,h</sup>, Kaigang Li<sup>i</sup>, Jongho Lee<sup>j</sup>, Phil Lee<sup>k</sup>, Se-Hong Oh<sup>l</sup>, Samantha Umland<sup>a</sup>, Michael L Thomas<sup>m</sup>

<sup>a</sup> The BRAiN lab, Department of Human Development and Family Studies/Molecular, Cellular and Integrative Neurosciences, Colorado State University, Fort Collins, CO, USA

<sup>b</sup> Department of Computer Science, Colorado State University, Fort Collins, CO, USA

<sup>c</sup> Marcus Institute for Brain Health, University of Colorado Anschutz Medical Campus, Aurora, CO, USA

<sup>d</sup> Department of Psychiatry and Behavioral Sciences, University of New Mexico School of Medicine, Albuquerque, NM, USA

<sup>e</sup> Tri-institutional Center for Translational Research in Neuroimaging and Data Science (TReNDS), Georgia State, Georgia Tech, Emory, Atlanta, GA, USA

<sup>f</sup> Department of Neurology, Department of Radiology, Hoglund Biomedical Imaging Center, University of Kansas Medical Center, Kansas City, KS, USA

<sup>g</sup> Beckman Institute for Advanced Science and Technology at the University of Illinois, IL, USA

<sup>h</sup> Center for Cognitive & Brain Health, Northeastern University, Boston, MA, USA

<sup>i</sup> Department of Health and Exercise Science, Colorado State University, Fort Collins, CO, USA

<sup>j</sup> Department of Electrical and Computer Engineering, Seoul National University, Seoul, Republic of Korea

<sup>k</sup> Department of Radiology, Hoglund Biomedical Imaging Center, University of Kansas Medical Center, Kansas City, KS, USA

<sup>l</sup> Division of Biomedical Engineering, Hankyong University of Foreign Studies, Gyeonggi-do, Republic of Korea

<sup>m</sup> Michael Thomas, Department of Psychology, Colorado State University, Fort Collins, CO, USA

### ARTICLE INFO

#### Keywords:

Metabolic syndrome  
White matter  
Aging  
Adiposity  
Myelin

### ABSTRACT

Metabolic syndrome (MetS) is a cluster of conditions that affects ~25% of the global population, including excess adiposity, hyperglycemia, dyslipidemia, and elevated blood pressure. MetS is one of major risk factors not only for chronic diseases, but also for dementia and cognitive dysfunction, although the underlying mechanisms remain poorly understood. White matter is of particular interest in the context of MetS due to the metabolic vulnerability of myelin maintenance, and the accumulating evidence for the importance of the white matter in the pathophysiology of dementia. Therefore, we investigated the associations of MetS risk score and adiposity (combined body mass index and waist circumference) with myelin water fraction measured with myelin water imaging. In 90 cognitively and neurologically healthy adults (20–79 years), we found that both high MetS risk score and adiposity were correlated with lower myelin water fraction in late-myelinating prefrontal and associative fibers, controlling for age, sex, race, ethnicity, education and income. Our findings call for randomized clinical trials to establish causality between MetS, adiposity, and myelin content, and to explore the potential of weight loss and visceral adiposity reduction as means to support maintenance of myelin integrity throughout adulthood, which could open new avenues for prevention or treatment of cognitive decline and dementia.

### 1. Introduction

Diagnosis of metabolic syndrome (MetS) is defined co-occurrence of at least three of the following conditions: excess abdominal fat (visceral adiposity), elevated fasting blood glucose, elevated blood pressure (BP),

and abnormal blood cholesterol or triglyceride levels [1]. In addition to increased risk of cardiovascular disease, type 2 diabetes, stroke, cancer, and overall mortality [2], MetS is also a known risk factor for Alzheimer's disease, vascular dementia, and cognitive dysfunction [3,4]. About 20–25% of global population is estimated to be affected by MetS

\* Corresponding author at: Department of Human Development and Family Studies, Molecular, Cellular and Integrative Neurosciences, Colorado State University, Campus Delivery 1570, Fort Collins, CO 80523-1570.

E-mail address: [agaburza@colostate.edu](mailto:agaburza@colostate.edu) (A.Z. Burzynska).

<sup>1</sup> Except the first author, all other authors are listed in alphabetic order.

<https://doi.org/10.1016/j.cccb.2023.100180>

Received 14 April 2023; Received in revised form 11 August 2023; Accepted 17 August 2023

Available online 19 August 2023

2666-2450/© 2023 The Authors. Published by Elsevier B.V. This is an open access article under the CC BY-NC-ND license (<http://creativecommons.org/licenses/by-nc-nd/4.0/>).

[5,6], but even a larger number of adults have pre-MetS, defined as presence at least two of the MetS components [7]. For instance, according to the World Health Organization (WHO), worldwide obesity rates tripled from 1975 to 2016 and 39% of adults were overweight and 13% were obese in 2016 [8]. Thus, MetS needs to be considered not only as a major public health problem, but also as a major modifiable risk for dementia. Therefore, this study aimed to understand the association of MetS with adult brain health.

Brain imaging studies have associated individual MetS components (i.e., hypertension, obesity, dyslipidemia, glucose intolerance) with lower global brain volumes, silent infarcts, white matter hyperintensities, and reduced gray matter density in adults [9,10]. However, little is known about MetS in relation to other metrics of brain health. The brain's white matter (WM) is of particular interest in the context of MetS, as the metabolic burden of myelin maintenance and repair makes WM particularly vulnerable to metabolic, inflammatory, and vascular stress, which accumulate with age [11] and are aggravated by each of the MetS components [9]. Indeed, brain tissue of Alzheimer's disease patients shows considerable mitochondrial malfunction, impaired energy metabolism, and chronic oxidative stress [12].

As reviewed by Alfaro et al. [9], MetS diagnosis as well as abnormalities of each MetS component have been linked to reduced microstructural integrity in multiple WM regions, especially in the frontotemporal regions, association fibers, and the corticospinal tract as evidenced by diffusion tensor imaging (DTI). DTI quantifies the overall magnitude and directionality of water diffusivity within each voxel, which depends on multiple microstructural white matter properties, with myelin being just one of them. Accordingly, DTI provides only an indirect measure of myelin integrity [13]. Therefore, findings linking MetS to white matter need to be validated using magnetic resonance imaging (MRI) measures that are more specific to myelin.

Myelin water imaging (MWI) utilizes the short T<sub>2</sub>-relaxation of the so-called "myelin water" (i.e., the water molecules between the lipid bilayers of the myelin sheath, both in myelin's cytoplasm and in extracellular space within the compacted myelin) to estimate myelin volume fraction (MWF) per voxel [14]. To date, only one recent study utilized MWI to understand the association of a single MetS component – adiposity – with brain's myelin. Specifically, Bouhrara and colleagues [15] showed that greater BMI and waist circumference (WC) were both related to lower myelin content in multiple WM regions in 119 cognitively healthy adults of aged 22–94 years, controlling for age, sex, and ethnicity. These findings are in line with earlier DTI studies reporting a negative association between adiposity and DTI measures of WM integrity [16–20]. Yet, these promising findings need to be replicated in independent samples and extended to other components of MetS.

Our primary hypothesis was that a greater risk of MetS would be associated with lower MWF in cognitively and neurologically healthy adults. Given the selective vulnerability of late-myelinating regions, known as the "retrogenesis", "last-in-first-out", or "development-to-degeneration" model of selective WM aging [11,21,22], we hypothesized that prefrontal WM and association fibers would exhibit the strongest negative associations with MetS risk score. In the aforementioned review of DTI findings [9], multiple studies reported associations of MetS-score or its components in the late-myelinating regions, but the retrogenesis pattern of selective vulnerability was not discussed. Our secondary aim was to verify the adiposity-MWF association reported by Bouhrara et al. [15] using 1) a different method for estimation MWF (i.e., the ratio of myelin water signal to total water signal based on the T<sub>2</sub> distribution), 2) a different data processing method and definition of WM regions, 3) a different definition of WC (measured at the superior border of the iliac crest compared to measuring the smallest point between the last floating rib and the superior border of the iliac crest) and 4) an extended set of covariates (e.g., race, education, and income) that are known to be associated with the incidence of MetS. Given the earlier finding that BP explained most of the variance in the association between adiposity (combined BMI and WC) and DTI-derived fractional

anisotropy [19], we tested whether the adiposity-MWF relationship is independent of systolic BP. Finally, we explored bivariate associations between all MetS components and regional MWF values.

## 2. Methods

### 2.1. Participants

Capacity to give informed consent was assessed using the decisional capacity approach [23] and the study was approved by the Colorado State University institutional review board. Participants were recruited from the Fort Collins area using social media (e.g., Nextdoor), word of mouth, mailing lists of several organizations (e.g., Osher Lifelong Learning Institute), and posters or flyers at local gyms or community centers (e.g., Fort Collins Senior Center).

Inclusion criteria included the ability to give informed consent and age 20–80 years. Exclusion criteria were designed to define homogenous and neurologically, psychiatrically, and cognitively healthy adult sample. We used exclusion criteria published in detail for the Human Connectome Project in Aging (HCP-A; [24]). Among the exclusions yielded by this approach were: a history of neurological and neurodegenerative diseases (e.g., Alzheimer's disease and related dementias, moderate to severe traumatic brain injury, brain tumor, brain surgery, stroke, multiple sclerosis, Parkinson's disease, epilepsy); psychiatric disorders (e.g. schizophrenia, bipolar disorder, substance dependence, severe depression); substance dependence; hearing or vision impairment, including macular degeneration; heart attack; thyroid problems; severe organ disease or failure; genetic disorder such as cystic fibrosis; medicated migraines; long-term use of steroids or immunosuppressants; changes in medication in the past year; or MRI safety contraindications (e.g., MRI-unsafe metals or devices in the body, moderate to severe claustrophobia, pregnancy).

To minimize the risk of inclusion of adults with cognitive impairment, we used a cutoff score of < 30 on modified Telephone Interview of Cognitive Status (TICS-M) questionnaire during phone screening [25], followed by in-person administration of the Mini-Mental State Examination (MMSE) [26], with exclusion resulting from performance one or more standard deviations below age- and education-based performance expectations (i.e., norms) [27]; Clinical Dementia Rating (CDR; excluded if > 0; [28]) and the short form of Geriatric Depression Scale (GDS-15; excluded if > 10; [29]); and < 9 years of education (to minimize the confounding effect lower educational attainment on MMSE performance). To further minimize the risk of neurological comorbidities linked with common vascular and metabolic conditions that can affect healthy WM aging (e.g., early stages of small vessel disease), we added the following exclusion criteria to the HCP-A list: smoking > 20 cigarettes or joints/month, mean resting systolic blood pressure > 140 [30], body mass index (BMI) > 33 [31,32], and > 2 on the modified Hachinski ischemic scale [33]. In addition, based on our experience, exclusion criterion of BMI > 33 helped us avoid situations when a participant cannot be comfortably placed in the scanner or is at risk of high specific absorption rate, especially when using work-in-progress sequences. Finally, participants would be excluded from the analyses if the anatomical scans would indicate brain abnormality, including, for example, WM hyperintensity burden greater than typical for participant's age, such as indicating vascular dementia.

The data presented here was collected as a part of an ongoing cross-sectional study and the data for the current analyses were drawn on 14th November 2022 (see Appendix A for the subject flow). Potential volunteers were screened during a phone interview. Next, if potential volunteers were qualified, they were scheduled for a 3-hour visit 1 during which we collected: signature of informed consent, MMSE, waist and hip circumference, ambulatory blood pressure, two cognitive batteries the Virginia Cognitive Aging Project battery (VCAP) [34] and the NIH Toolbox® Cognition for ages 8+ [35,36] and a brief questionnaire on health history, lifestyle, socioeconomic factors, and family history of

dementia. After visit 1 each participant was given an ActiGraph accelerometer to wear for 7–10 days (data not reported in the current study) and to be returned during the MRI session (visit 2), during which we measured height and weight.

## 2.2. MRI acquisition

Imaging was performed on a 3T MRI system (Siemens MAGNETOM Skyra) with a 64-channel RF coil. The acquisition session was part of an ongoing study and therefore included multiple MRI sequences, of which the multi-echo T2 relaxation imaging was used in this study. At the time of data analysis, 96 datasets were collected, out of which six had missing MWI data due to technical issues. Fluid attenuated inversion recovery (FLAIR) sequence was used to screen for clinically significant WM abnormalities (TE/TI/TR = 387/1800/5000 ms, Field of view (FOV) = 230 mm, resolution = 0.9 mm<sup>3</sup>, 192 slices, GRAPPA acceleration factor 2). Multi-echo T2 relaxation images were acquired in the transverse plane with a 3D-gradient and spin-echo (GRASE) sequence. The duration of the GRASE sequence was 10.03 min (TR = 1000 ms, first TE = 10 ms, echo spacing = 10 ms, number of echoes = 32, FOV = 240 mm, resolution = 1.9 × 1.9 × 4.0 mm<sup>3</sup>, 32 slices). Diffusion-weighted images were acquired using a multi-shell ( $b = 0, 1000, 2000\text{s/mm}^2$ ) high-angular-resolution (138 directions) multiband echo planar sequence in transversal plane (TE/TR = 104.8/3120 ms, FOV = 234 mm, resolution = 1.8 mm<sup>3</sup>, 76 slices, multiband acceleration factor = 4, flip angle 79°, refocus flip angle 160°). The scan was repeated for both anterior-to-posterior and posterior-to-anterior phase encoding directions, each lasting 7.31 min.

## 2.3. Image analysis and registration

3D GRASE images were fitted using an in-house script in Matlab [37]. In brief, we used fitting of multiple exponential functions with stimulated echo correction using an extended phase graph to generate a

T<sub>2</sub> distribution from the multi-echo data. To improve the reliability of the fitting, we used Tikhonov regularization, which enforces minimum energy and generates a smooth T<sub>2</sub> distribution. Finally, a myelin water fraction (MWF), which is the ratio of myelin water signal to total water signal, was calculated at each voxel. We used the integration ranges 10 ms – 40 ms for myelin water pool and 40 ms–2000 ms for the axonal/extracellular water pool.

Then, the first echo images from the 3D GRASE acquisition were linearly registered to the unwarped  $b = 0$  DWI maps (6 degrees of freedom), and this transformation was then applied to the individual MWF maps so that they were aligned with the  $b = 0$  images, and, therefore, with FA images (Fig. 1).

From the pairs of the DWIs acquired with reversed phase-encoding blips, susceptibility-induced off-resonance field was estimated [38], as implemented in FSL as *topup* [39], generating a single corrected (or unwarped)  $b = 0$  image. Then, the *topup* distortion correction was applied using *eddy* in FSL [40], which also corrected for distortions related to eddy current and motion. The diffusion tensor model was fitted to the data using the FSL Diffusion Toolbox v.5.0 (FDT), yielding the fractional anisotropy (FA) maps. Finally, we used the tract-based spatial statistics (TBSS) [41] workflow in FSL v6.0.5.2. In brief, this included: (a) nonlinear alignment of each participant's FA volume to the 1 × 1 × 1 mm<sup>3</sup> standard Montreal Neurological Institute (MNI152) space via the FMRIB58\_FA template using the FMRIB's Nonlinear Registration Tool (FNIRT, [42]; [www.doc.ic.ac.uk/~dr/software](http://www.doc.ic.ac.uk/~dr/software)), (b) calculation of the mean of all aligned FA images, (c) creation of the WM "skeleton" (a representation of WM tracts common to all subjects) by perpendicular non-maximum-suppression of the mean FA image and setting the FA threshold to 0.2, (d) perpendicular projection of the highest FA value (local center-of-tract) onto the skeleton, separately for each subject, and (e) application of *tbss\_non\_FA* procedure to MWF maps aligned with the unwarped  $b = 0$  images, yielding MWF values projected on the skeleton. MWF values represent a fraction with the range 0–1. All steps of image processing and registration for all participants were

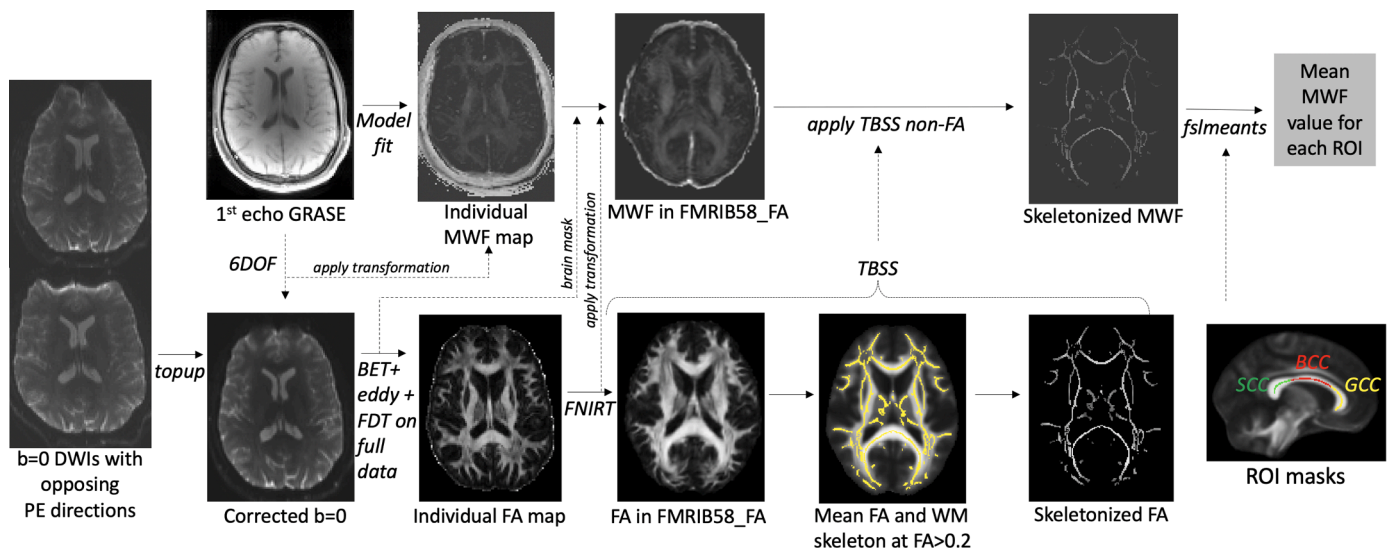


**Fig. 1.** Image processing pipeline. From left to right: First, pairs of  $b=0$  diffusion-weighted images (DWIs) acquired in opposite phase encoding (PE) directions were subjected to *topup* in FSL, which resulted in a susceptibility distortion-corrected  $b=0$  images. These corrected images were then averaged and subjected to *brain extraction tool* (BET) in FSL to remove non-brain tissue, followed by *eddy* procedure, yielding unwarped and motion-corrected DWI data. Diffusion tensor model was then fitted to the data using FSL Diffusion Tool (FDT), followed by the Tract-Based Spatial Statistics (TBSS) procedure, which included non-linear registration to the FMRIB58\_FA template, creation of the sample's mean FA image, distance map (not shown), the WM skeleton, and, finally, projection of the center-of tract FA values to the skeleton for all participants. Next, individual GRASE data were fitted to obtain MWF maps. The 1st echo GRASE images were linearly registered to the corrected  $b=0$  DWIs, and this transformation was then applied to the MWF map. The brain mask (generated during DWI processing) was then applied to the MWF map aligned to  $b=0$  image to remove non-brain tissue. Next, the brain-extracted MWF maps were subjected to the TBSS non-FA procedure, which applied the previously estimated nonlinear transformations to the FMRIB58\_FA and projected the MWF values on the skeleton. Finally, regional MWF values were obtained by averaging MWF values within each region of interest (ROI). Example ROIs: BCC: body of CC, GCC: genu CC, SCC: splenium CC; FNIRT: FSL non-linear registration tool.

visually inspected in either FSLeves or by using slicesdir command.

#### 2.4. Regions of interest

To estimate myelin content in the entire WM, we averaged the MWF values from the entire skeleton for each participant (whole WM). Next, we extracted mean MWF values from regions (Table 1) representing the major association, projection, and commissural fibers, as described previously [43], using the DTI white-matter atlas [44], with the aim to include the core regions specific to each tract. The corpus callosum was segmented so that genu representing prefrontal commissural fibers, body containing premotor, supplementary motor, motor and sensory fibers, and splenium containing parietal, temporal and occipital connections [45]. The prefrontal WM region was defined as  $y > 12$  in MNI coordinate space and whole WM included the whole TBSS skeleton. The cingulum included both the ventral and dorsal segments, and the corticospinal tract was represented by the core regions of the superior corona radiata, posterior limb of the internal capsule, and the cerebral peduncles. The uncinate was probed in the lateral ventral prefrontal region as well as in the section along the fronto-occipital fasciculus. Mean MWF was extracted from each region using *fslmeants* in FSL.

#### 2.5. Indicators of metabolic syndrome risk

Ambulatory blood pressure (BP) was measured during visit 1 (about 2 weeks before MRI during visit 2) using the Bronze Omron upper arm digital automatic monitor (BP5100). First, the participant was seated and asked to fill in the study documentation for at least 5 min. Then, a measurement was taken from both arms, while making sure the participant is not talking or crossing their legs. The arm with the higher measurement was noted and chosen for subsequent measurements. Following the American Heart Association guidelines [46], we recorded three BP measurements, 1 min apart, using the selected arm. Additional

**Table 1**  
Descriptive statistics.

|                   | Min     | Max      | M         | SD    |
|-------------------|---------|----------|-----------|-------|
| Age (years)       | 20.0    | 79.0     | 52.8      | 17.7  |
| MMSE              | 27.0    | 30.0     | 29.4      | 0.7   |
| Education (years) | 11.0    | 22.0     | 17.0      | 2.6   |
| Income (\$/year)  | <30,000 | >120,000 | >120,000* | 1.7   |
| Systolic BP       | 96.2    | 151.0    | 121.3     | 12.3  |
| Diastolic BP      | 60.0    | 100.3    | 78.5      | 7.2   |
| WC (cm)           | 70.0    | 122.0    | 94.9      | 11.4  |
| Height (m)        | 1.52    | 1.91     | 1.68      | 0.1   |
| Weight (kg)       | 48.1    | 110.2    | 71.7      | 12.5  |
| BMI               | 19.0    | 32.7     | 25.4      | 3.5   |
| <i>MWF</i>        |         |          |           |       |
| Whole WM          | 0.059   | 0.121    | 0.090     | 0.014 |
| Prefrontal WM     | 0.018   | 0.106    | 0.056     | 0.020 |
| Genu CC           | 0.019   | 0.147    | 0.079     | 0.027 |
| Body CC           | 0.030   | 0.14     | 0.093     | 0.021 |
| Splenium CC       | 0.064   | 0.180    | 0.130     | 0.021 |
| mPFC              | 0.001   | 0.114    | 0.041     | 0.022 |
| UNC               | 0.010   | 0.100    | 0.035     | 0.021 |
| SLF               | 0.066   | 0.145    | 0.102     | 0.017 |
| CING              | 0.020   | 0.120    | 0.065     | 0.021 |
| FX                | 0.020   | 0.110    | 0.063     | 0.018 |
| EC                | 0.011   | 0.103    | 0.042     | 0.019 |
| TEMP              | 0.025   | 0.103    | 0.055     | 0.016 |
| CST               | 0.120   | 0.240    | 0.165     | 0.021 |
| ALIC              | 0.046   | 0.202    | 0.113     | 0.034 |

Note:  $N = 90$  for all variables. MMSE: mini-mental state examination, BP: blood pressure, WC: waist circumference, BMI: body mass index, MWF: myelin water fraction, WM: white matter, CC: corpus callosum, external capsule (EC), fornix (FX), superior longitudinal fasciculus (SLF), anterior limb of the internal capsule (ALIC), cingulum bundle (CING), uncinate fasciculus (UNC), WM of the medial PFC (mPFC), WM of the temporal pole related to inferior longitudinal fasciculus (TEMP), and corticospinal tract (CST). \*Median/mode.

measurements were taken only if the first two readings differed by  $> 10$  mmHg. We used an average of the last two BP readings to estimate each individual's systolic and diastolic BP. Only participants who had mean systolic BP  $< 140$  were included in this study (those who did not pass were discontinued and further data was not collected). Participants were asked to follow their morning routine before coming to visit 1, such as including breakfast and coffee, to feel comfortable.

WC were collected using measurement tape according to WHO [47] guidelines. Specifically, the waist was defined as the superior border of the iliac crest. WC was used to classify participants into lean ( $< 80$  cm for women,  $< 94$  cm for men), overweight (80–88 cm for women, 94–102 cm for men), and obese ( $> 88$  cm for women,  $> 102$  cm for men; [48]). Weight and height were collected prior to the MRI scan, using vertical tape mounted on the wall, and a Rivio electronic personal scale. BMI was calculated by converting the measurements to metric units and then dividing the weight of the participant by their squared height. BMI  $< 18.5$  was classified as underweight, 18.5–25 as healthy weight (lean), 25–30 as overweight, and  $> 30$  as obese [48].

Participants were asked to respond “yes” or “no” to the following questions: “Has a doctor ever told you your cholesterol level was high?” and “Has a doctor ever told you your blood sugar levels (glucose) were high?”.

To assess the continuum of metabolic and cardiovascular risk factors, we computed a “MetS risk score” as a combination of systolic BP, waist circumference, BMI, and a history of abnormal blood cholesterol or fasting glucose results. We found this new approach more suitable in our healthy (or above average healthy) adult sample that the binary MetS diagnosis (see Appendix B), given that our study criteria excluded participants with stage 2 hypertension (systolic  $> 140$ ), more severe obesity (BMI  $> 33$ ), and elevated ischemic risk. In addition, MetS binary diagnosis is designed for people 24 and older [1], yet given the increasing rates of obesity and cardiovascular disease in the young population and its importance for brain health, our study included participants of age 20–24. The MetS risk score was computed by adding the z-scored values of mean systolic BP, WC, BMI, and self-reported history of elevated cholesterol and sugar (one missing value for WC was replaced with sample mean). Additionally, we calculated the adiposity score by adding the z-scored values of BMI and WC, similar to what was done in an earlier study relating adiposity to DTI measures [19]. Also, given that BMI and WC showed similar associations with MWF [15], combining the two measures allowed us to reduce the number of statistical tests.

#### 2.6. Covariates

The prevalence of MetS, obesity, hypertension, diabetes and risks of cardiovascular diseases varies by race and ethnicity (i.e., lowest among non-Hispanic whites) and correlates with lower income and lower education [49], especially among women [50]. Thus, we included sex, years of education, income, race and ethnicity as covariates in all analyses. Household income information was collected as 1:  $< \$30,000$ ; 2:  $\$30,000$ – $\$50,000$ ; 3:  $\$50,000$ – $\$70,000$ ; 4:  $\$70,000$ – $\$90,000$ ; 5:  $\$90,000$ – $\$120,000$ ; 6:  $\geq \$120,000$ .

#### 2.7. Statistical analyses

Bivariate correlations were used to assess the relationships of MWF with age and age<sup>2</sup>. The inclusion of age<sup>2</sup> as an independent variable is based on others' recent observations that myelination follows a quadratic relationship with age [15,51,52]. As these results are reported for the future meta-analyses, Table 2 includes raw p-values (not corrected for multiple comparisons). Effect sizes were as considered small ( $0.2 < r < 0.3$ ), medium ( $0.3 \leq r < 0.5$ ) or large ( $r \geq 0.5$ ) for both correlations and standardized  $\beta$  coefficients in regressions. Next, to test the main hypothesis that MWF is associated with MetS risk score, we conducted 14 linear regressions, with regional MWF as the dependent variable, and age, age<sup>2</sup>, sex, race, ethnicity, education, income, and

**Table 2**  
Linear and quadratic associations of MWF with age.

| WM region (MWF) |          | Age    | Age <sup>2</sup> |
|-----------------|----------|--------|------------------|
| Whole WM        | <i>r</i> | -0.16  | -0.20            |
|                 | <i>p</i> | 0.128  | 0.063            |
| Prefrontal WM   | <i>r</i> | -0.33  | -0.34            |
|                 | <i>p</i> | 0.002  | <0.001           |
| Genu CC         | <i>r</i> | -0.46  | -0.45            |
|                 | <i>p</i> | <0.001 | <0.001           |
| Body CC         | <i>r</i> | 0.21   | 0.20             |
|                 | <i>p</i> | 0.042  | 0.063            |
| Splenium CC     | <i>r</i> | 0.22   | 0.20             |
|                 | <i>p</i> | 0.037  | 0.054            |
| mPFC            | <i>r</i> | -0.29  | -0.30            |
|                 | <i>p</i> | 0.006  | 0.004            |
| UNC             | <i>r</i> | -0.16  | -0.18            |
|                 | <i>p</i> | 0.131  | 0.089            |
| SLF             | <i>r</i> | -0.22  | -0.25            |
|                 | <i>p</i> | 0.037  | 0.020            |
| CING            | <i>r</i> | -0.22  | -0.23            |
|                 | <i>p</i> | 0.040  | 0.027            |
| FX              | <i>r</i> | 0.18   | 0.17             |
|                 | <i>p</i> | 0.089  | 0.120            |
| EC              | <i>r</i> | 0.33   | 0.30             |
|                 | <i>p</i> | 0.001  | 0.005            |
| TEMP            | <i>r</i> | -0.19  | -0.21            |
|                 | <i>p</i> | 0.072  | 0.047            |
| CST             | <i>r</i> | -0.31  | -0.35            |
|                 | <i>p</i> | 0.003  | <0.001           |
| ALIC            | <i>r</i> | 0.18   | 0.13             |
|                 | <i>p</i> | 0.095  | 0.207            |

Note: All correlations were on *N* = 90; see Table 1 for other abbreviations. *P*-values are uncorrected.

MetS risk score as independent variables. In the regression models, to remove nonessential collinearity between age and age<sup>2</sup>, the age variable was centered by subtracting the group mean from each individual value, and age<sup>2</sup> was calculated from this centered variable. We reported both raw and FDR-corrected *p*-values. Similarly, to test whether adiposity is associated with MWF, we conducted 14 linear regressions, with regional MWF as the dependent variable, and age, age<sup>2</sup>, sex, race, ethnicity, education, income, systolic BP, and adiposity score as independent variables. We used bivariate two-tailed Pearson’s correlations to explore the associations between WC, BMI, systolic BP and regional MWF, and independent samples *t*-test to compare MWF between those with a history of dyslipidemia or hyperglycemia and those without. All analyses were conducted in SPSS v.28. and FDR correction was applied using the Benjamini-Hochberg method. FDR-corrected *p*-values of 0.05 or smaller were considered significant.

### 3. Results

#### 3.1. Sample characteristics

In this sample, 24.4% were men and 75.6% were women. Racial composition of the sample was 84% White, 1.1% Asian, 1.1% American Indian/Alaskan, 2.2% “more than one race,” and 2.2% unknown/did not respond. Next, 91.1% identified as not Hispanic/Latino and 8.9% as Hispanic/Latino. 40% reported having a history of elevated cholesterol and 10% having a history of elevated blood sugar. BMI identified 50% of the sample as lean, 36.7% as overweight, and 13.3% as obese. According to sex-adjusted WC, 12.2% were lean, 30% were overweight, and 56.7% were obese. Table 1 describes other sample characteristics.

#### 3.2. Myelin water fraction: age and sex differences

First, we investigated the associations of MWF with age and sex, given that MWI studies on healthy aging are still scarce. Table 1 reports mean MWF values for each WM region. Mean MWF was the highest in the early-myelinating cerebrospinal tract (~16%), and splenium CC,

and the lowest in the late-myelinating uncinate (~3.5%), medial PFC (~4.1%) and external capsule (4.2%).

Table 2 shows region-specific linear and quadratic correlations of MWF with age. Negative associations of medium effect size were observed in the genu CC, prefrontal WM, corticospinal tract, and medial prefrontal WM. Negative associations of small effect size were observed in the whole WM, superior longitudinal fasciculus, cingulum bundle, and temporal WM. We also observed medium effect size positive associations in the external capsule. Together, our findings support using both age and age<sup>2</sup> as covariates in the subsequent regression models.

In addition, Appendix C shows mean MWF values for each region, broken down by age decade, as a reference for future meta-analyses and comparative studies. Appendix D contains the results of the two-way ANOVA analyzing the main effects of sex, a decade of life, and sex \* decade interaction, as well as the descriptive statistics for MWF values broken down by sex and decade. In brief, there was no significant effect of sex or sex \* decade interaction for any of the WM regions. Therefore, mean MWF values reported in Table 1 and Appendix C represent both sexes. Similar to the univariate correlations in Table 2, two-way ANOVA showed a significant effect of age decade, age-related decreases in MWF in medial prefrontal WM, genu CC, and corticospinal tract, and an increase in MWF in the external capsule.

#### 3.3. Associations of MetS score with myelin water fraction

Table 3 shows regression relationships between MetS score and MWF. Medium effect size negative relationships were observed in the uncinate fasciculus, prefrontal WM, and medial prefrontal WM (Fig. 2), whereas small effect size negative associations were present in the whole WM, genu CC, whole WM, fornix, external capsule, corticospinal tract and the anterior limb of the internal capsule (not significant after FDR correction).

#### 3.4. Adiposity and myelin water fraction

Table 4 shows the outcomes of the linear regression relating adiposity to regional MWF, after controlling for age, age<sup>2</sup>, sex, race, ethnicity, income, education, and systolic BP. In brief, adiposity showed large effect size negative association with brain’s myelin in the uncinate, and medium effects size negative associations in the prefrontal WM, medial prefrontal WM, genu CC, the external capsule, fornix, and the whole WM (Fig. 2). There were also negative associations with small effect size in the superior longitudinal fasciculi and corticospinal tract

**Table 3**

Associations between MetS and MWF, controlling for age, age<sup>2</sup>, sex, race, ethnicity, education and income.

| WM region        | Std. $\beta$ | <i>t</i> | <i>p</i><br>uncorrected | <i>p</i> FDR-<br>corrected | Overall regression<br>model fit   |          |
|------------------|--------------|----------|-------------------------|----------------------------|-----------------------------------|----------|
|                  |              |          |                         |                            | Adjusted<br><i>R</i> <sup>2</sup> | <i>p</i> |
| Whole WM         | -0.22        | -1.74    | 0.086                   | 0.241                      | 0.05                              | 0.132    |
| Prefrontal<br>WM | -0.37        | -3.02    | 0.003                   | 0.021                      | 0.15                              | 0.005    |
| Genu CC          | -0.27        | -2.35    | 0.021                   | 0.074                      | 0.23                              | <0.001   |
| Body CC          | 0.06         | 0.42     | 0.677                   | 0.862                      | 0.01                              | 0.358    |
| Splenium<br>CC   | 0.03         | 0.23     | 0.822                   | 0.959                      | 0.06                              | 0.115    |
| mPFC             | -0.32        | -2.62    | 0.011                   | 0.051                      | 0.17                              | 0.003    |
| UNC              | -0.47        | -3.94    | <0.001                  | <0.014                     | 0.17                              | 0.003    |
| SLF              | -0.18        | -1.41    | 0.161                   | 0.282                      | 0.06                              | 0.109    |
| CING             | 0.09         | 0.73     | 0.469                   | 0.730                      | 0.04                              | 0.185    |
| FX               | -0.28        | -2.12    | 0.037                   | 0.173                      | 0.01                              | 0.355    |
| EC               | -0.21        | -1.73    | 0.087                   | 0.203                      | 0.16                              | 0.005    |
| TEMP             | -0.09        | -0.68    | 0.500                   | 0.700                      | 0.06                              | 0.122    |
| CST              | -0.25        | -2.12    | 0.037                   | 0.173                      | 0.19                              | 0.002    |
| ALIC             | -0.21        | -1.62    | 0.110                   | 0.220                      | 0.08                              | 0.058    |

Note: Degrees of freedom: 8/80.

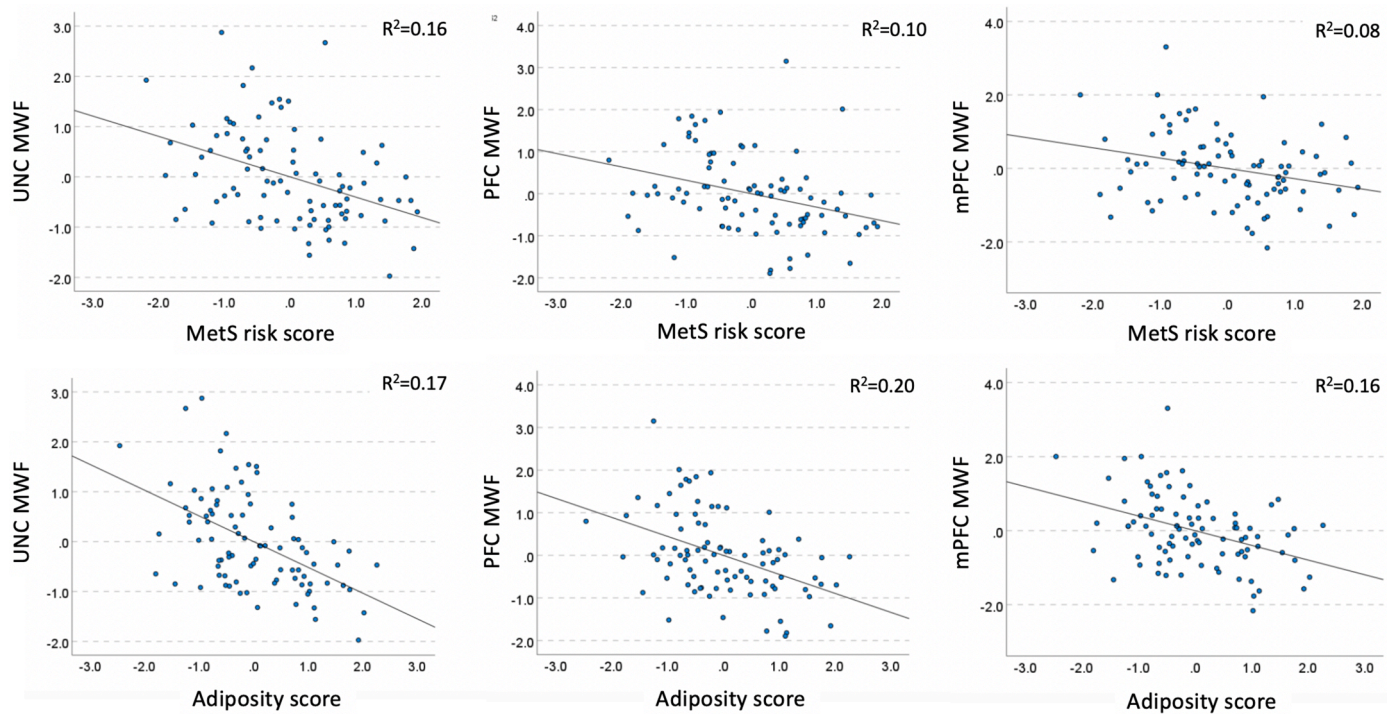


Fig. 2. Partial regression plots showing associations of MetS risk and adiposity scores and MWF shown in Tables 3 and 4. The standardized residuals of both predictor variables (MetS or adiposity) and dependent (regional MWF) were obtained by regressing the variable against age, age<sup>2</sup>, sex, race, ethnicity, education, and income. UNC: uncinate fasciculus, PFC: prefrontal WM, mPFC: medial prefrontal WM.

Table 4

Associations between adiposity and MWF, controlling for age, age<sup>2</sup>, sex, race, ethnicity, education, income, and systolic BP.

| WM region     | Std. $\beta$ | $t$   | Raw $p$ | FDR-corrected $p$ | Overall regression model fit |        |
|---------------|--------------|-------|---------|-------------------|------------------------------|--------|
|               |              |       |         |                   | Adjusted R <sup>2</sup>      | $p$    |
| Whole WM      | -0.31        | -2.47 | 0.016   | 0.112             | 0.08                         | 0.066  |
| Prefrontal WM | -0.48        | -4.18 | <0.001  | <0.014            | 0.24                         | <0.001 |
| Genu CC       | -0.43        | -3.92 | <0.001  | <0.014            | 0.31                         | <0.001 |
| Body CC       | -0.11        | -0.86 | 0.395   | 0.691             | 0.03                         | 0.231  |
| Splenium CC   | -0.11        | -0.85 | 0.397   | 0.617             | 0.07                         | 0.109  |
| mPFC          | -0.41        | -3.62 | <0.001  | <0.014            | 0.23                         | <0.001 |
| UNC           | -0.55        | -4.94 | <0.001  | <0.014            | 0.26                         | <0.001 |
| SLF           | -0.26        | -2.07 | 0.042   | 0.147             | 0.08                         | 0.073  |
| CING          | -0.10        | -0.75 | 0.454   | 0.636             | 0.03                         | 0.246  |
| FX            | -0.31        | -2.36 | 0.021   | 0.098             | 0.02                         | 0.332  |
| EC            | -0.42        | -3.70 | <0.001  | <0.014            | 0.25                         | <0.001 |
| TEMP          | -0.16        | -1.25 | 0.214   | 0.428             | 0.06                         | 0.125  |
| CST           | -0.22        | -1.86 | 0.067   | 0.188             | 0.20                         | 0.001  |
| ALIC          | -0.18        | -1.46 | 0.149   | 0.349             | 0.09                         | 0.062  |

Note: Degrees of freedom: 9/79.

(not significant after FDR correction). Adding systolic BP as an additional covariate had virtually no effect on the adiposity-MWF association (see the model without systolic SB in Appendix F for comparison).

### 3.5. Exploratory associations

Bivariate 2-tailed correlations between BMI, WC, and systolic BP revealed a complex pattern of region-specific associations (Table 5). For both WC and BMI, negative correlations with medium effect size were observed for fiber tracts and regions associated with the prefrontal cortex (prefrontal and medial prefrontal WM, genu, genu CC, uncinate), consistent with the results using the summary adiposity score in Table 4.

Table 5

Exploratory bivariate associations between BMI, WC and systolic BP with MWF.

| Regional MWF  |     | BMI    | WC     | Systolic BP |
|---------------|-----|--------|--------|-------------|
| WC            | $R$ | 0.65   |        |             |
|               | $p$ | <0.001 |        |             |
| Systolic BP   | $r$ | 0.32   | 0.46   |             |
|               | $p$ | 0.002  | <0.001 |             |
| Whole WM      | $r$ | -0.16  | -0.27  | -0.08       |
|               | $p$ | 0.129  | 0.009  | 0.449       |
| Prefrontal WM | $r$ | -0.42  | -0.45  | -0.22       |
|               | $p$ | <0.001 | <0.001 | 0.038       |
| Genu CC       | $r$ | -0.47  | -0.44  | -0.23       |
|               | $p$ | <0.001 | <0.001 | 0.031       |
| Body CC       | $r$ | 0.08   | 0.08   | 0.29        |
|               | $p$ | 0.484  | 0.451  | 0.005       |
| Splenium CC   | $r$ | 0.07   | -0.003 | 0.21        |
|               | $p$ | 0.498  | 0.980  | 0.047       |
| mPFC          | $r$ | -0.35  | -0.45  | -0.22       |
|               | $p$ | <0.001 | <0.001 | 0.036       |
| UNC           | $r$ | -0.38  | -0.49  | -0.22       |
|               | $p$ | <0.001 | <0.001 | 0.035       |
| SLF           | $r$ | -0.15  | -0.25  | -0.10       |
|               | $p$ | 0.160  | 0.017  | 0.352       |
| CING          | $r$ | -0.04  | -0.06  | 0.01        |
|               | $p$ | 0.711  | 0.552  | 0.910       |
| FX            | $r$ | -0.20  | -0.13  | 0.01        |
|               | $p$ | 0.056  | 0.227  | 0.936       |
| EC            | $r$ | -0.01  | -0.18  | 0.12        |
|               | $p$ | 0.365  | 0.096  | 0.264       |
| TEMP          | $r$ | -0.07  | -0.17  | -0.09       |
|               | $p$ | 0.507  | 0.113  | 0.400       |
| CST           | $r$ | -0.14  | -0.26  | -0.24       |
|               | $p$ | 0.196  | 0.013  | 0.023       |
| ALIC          | $r$ | -0.06  | -0.15  | -0.08       |
|               | $p$ | 0.601  | 0.156  | 0.457       |

There were also small effect size negative (and mostly quadratic) associations of WC and BMI with myelin in the whole WM, fornix, superior longitudinal fasciculus, and corticospinal tract. Small effect size

negative correlations of systolic BP and myelin were observed in the prefrontal and medial prefrontal WM, genu, genu CC, uncinata, and the corticospinal tract. In addition, there were small effect size positive associations between systolic BP and myelin in the body and splenium of the CC.

For dichotomous variables (history of hyperglycemia or dyslipidemia), we performed independent t-tests. In prefrontal WM ( $p = .007$ ,  $d = 0.60$ ), genu CC ( $p < .001$ ,  $d = 0.80$ ), and SLF ( $p = .032$ ,  $d = 0.49$ ) participants reporting a history of elevated blood cholesterol had lower MWF than those without. We found no difference in MWF between those with a history of elevated blood glucose and those without (all  $p$ -values  $> 0.150$ , for details such as descriptive statistics, see Appendix E).

#### 4. Discussion

The current study investigated the associations between MetS and its components with myelin water fraction in the white matter of cognitively and neurologically healthy adults. Our main findings are: 1) MetS risk score was correlated with lower MWF in the uncinata fasciculi and prefrontal WM, controlling for age, age<sup>2</sup>, sex, race, ethnicity, education and income; 2) Adiposity, consisting of BMI and WC, was negatively associated with MWF in the uncinata, prefrontal WM, medial PFC WM, genu CC, and the external capsule, controlling for age, age<sup>2</sup>, sex, race, ethnicity, education and income; and 3) The adiposity-MWF association was independent of systolic BP. In addition, we reported regional variability in MWF values, linear and quadratic correlations of MWF with age, which are consistent with earlier reports using quantitative MRI and MWI [15,51–54].

##### 4.1. MetS risk scores and MWF in late-myelinating regions

We provide here the first evidence for the association of MetS score with decreased myelin fraction in healthy adults. This finding is significant, as it indicates that the previously observed microstructural alterations related to MetS diagnosis or its individual components (as summarized in [9]) are, at least partly, attributed to decreased myelin content. Our study is, for example, aligned with a previous DTI investigation that reported a synergistic effect of subclinical elevation in several MetS risk indicators scores on greater within-person declines in fractional anisotropy and increases in radial diffusivity in a comparable sample of healthy adults [55].

The associations were most evident in prefrontal WM and uncinata fasciculus, an association tract that connects the anterior temporal and inferior frontal lobes. These tracts are known to be phylogenetically and ontogenetically late-myelinating. For instance, WM of the temporal and frontal poles begins to myelinate after the age of two and the most intensive myelination in the corpus callosum occurs at ages 2–7 [56]. Then, myelination progresses slowly over decades, reaching a peak in the fourth and fifth decade of life, as estimated with several quantitative MRI techniques; myelination seems to be especially protracted in the uncinata fasciculus [52,57].

Late myelinating WM regions are characterized by a lower oligodendrocyte-to-axon ratio (up to 50-fold) in late-myelinating regions as compared to early-myelinating primary motor and sensory regions, different lipid properties, myelin turnover, and reduced capacity for myelin repair in late-myelinating regions, as well as thinner and structurally more vulnerable myelin sheaths, that are more susceptible to breakdown, as reviewed in [58,59]. Despite the overall lower myelin content [57] related to smaller axonal diameter [60], the late-myelinating anterior callosal fibers show the largest investments in myelination for a given axonal caliber [52]. Here, we provide one of the first evidence for MetS score, as a combination of metabolic and vascular risk factors, as a significant contributor to selective vulnerability of late-myelinating prefrontal and associative WM tracts in healthy adults.

The currently proposed mechanisms of action of MetS on brain tissue include neuroinflammation, oxidative stress, abnormal brain lipid

metabolism, or as well as hypoperfusion and impaired vascular reactivity. Furthermore, cerebral blood flow is known to be reduced in MetS [61], and whole-brain as well as regional cerebral blood flow is known to correlate with myelin content in healthy adults [62]. Although the exact mechanisms of action of MetS on myelin are unknown, all of the above processes limit the ability to maintain energy-dependent processes and clear metabolic waste [10] which is of particular importance for oligodendrocytes due to demands not only of myelination, but also providing metabolic support to the neurons [63]. For instance, oligodendrocytes deliver glycolysis products for mitochondrial ATP production to axons, as well as transport a variety of molecules from their soma to the periaxonal space via myelinic channels [64]. Oligodendrocytes are also coupled by gap junctions to astrocytes and, thus, indirectly, to the blood–brain barrier [63]. Thus, MetS may have a negative impact on oligodendrocyte function, which impairs not only myelin sheath structure, but also metabolic support to axons. Whether axonal survival is also impaired by MetS, needs to be verified using MRI methods allowing for quantification of axonal content.

The significance of our finding is also related to the high prevalence of MetS in the population. Our inclusion and exclusion criteria were stricter than typical for a healthy population, even with regard to general health. For example, we disqualified anyone with mean systolic BP  $> 140$ , BMI  $> 33$ , or elevated cardiovascular risks. Yet, 22% of our sample had possible MetS and 31% had possible pre-MetS (see Appendix B). Given that we did not measure blood glucose and lipids, these percentages were likely even higher. Thus, we argue that MetS may be one of the key modifiable risk factors for the adult WM. Given the increasingly appreciated role of the WM in the pathophysiology of the Alzheimer's disease [59,65], understanding the impact of MetS on WM may open new avenues for prevention and treatment.

##### 4.2. Adiposity and its components, and MWF

Bivariate correlations showed that both BMI and WC showed overlapping, negative associations with MWF, of medium effects size, consistent with recent findings [15]. BMI and WC were also strongly associated with each other, which justified combining them in regression analyses. Regression analyses replicated and extended the previous findings linking adiposity to MWF [15], despite using different MWI method (BMC-mcDESPOT vs. GRASE in our study) in an independent sample, additional covariates, and a different method for extracting regional MWF values.

The WM regions showing adiposity-MWF association in our study were restricted to prefrontal regions and late-myelinating association fibers, as compared with more widespread associations reported by Bouhrara and colleagues [15]. This could be explained by several differences in study methodology. For example, we extracted center-of-the-tract MWF data, which could have overestimated MWF values and underestimated the effects of MetS and adiposity on myelin (see more on this in 4.3. Limitations). Next, we used a different definition of WC, which was defined as the superior border of the iliac crest, where the abdominal circumference is typically the largest, whereas the World Health Organization defines the waist circumference as the smallest point between the last floating rib and the highest point of the iliac crest which could result in smaller measurements [47]. As a result, our sample showed a greater discrepancy between WC and BMI classification (BMI: 50% lean, 37% overweight, 13% obese; WC: 12% lean, 30% overweight, 57% obese), which was more aligned in the other sample (BMI: 43% lean, 44% overweight, 13% obese; WC: 56% lean, 28% overweight, 16% obese; [15]). However, when looking at the BMI cutoffs, our samples look very comparable, which is in line with similar inclusion/exclusion criteria that were used by both studies. Also, the two studies used different MWI method: ours was based on myelin water's shorter T2 signal, whereas the other group multicomponent MRI relaxometry, known also as steady-state-based MWI. Although both methods have certain advantages and limitations [14], our findings indicate that both

methods yielded converging results on associations with WC, BMI, as well as with chronological age.

The regression analyses using adiposity as an independent variable showed more widespread and larger effects sizes associations with myelin (Table 4) than with MetS risk score as the independent variable (Table 3) and the adiposity-MWF associations were not attenuated by controlling for systolic BP, despite some spatial overlap in bivariate correlations with MWF between BMI, WC, and systolic BP (Table 5). Together, these data suggest that adiposity is an important predictor of myelin content. This is in agreement with a large body of DTI studies reporting associations between different measures of adiposity and WM microstructure [9]. Furthermore, our results add to the ongoing discussion on the synergistic vs. independent effects of MetS components on WM. For example, we did not replicate the earlier DTI findings showing that BP was the only significant correlate of fractional anisotropy [66] or the mediator of adiposity-fractional anisotropy association [19]. However, this discrepancy regarding BP results could be due to the MRI methods, with MWF being more specific to myelin and fractional anisotropy depending on a combination of several microstructural properties, such as fiber coherence, axonal density, or water content. Our results were more aligned with an earlier finding of independent effects of BP, HDL cholesterol, triglycerides, and BMI on WM integrity measured with magnetization transfer rate, a measure of macromolecular content, which is largely driven by myelin content [67].

While the exact mechanisms linking adiposity to myelin content remain to be identified, they likely overlap with those mentioned above for MetS, and include, among others, low-grade chronic inflammation, disrupted energy balance regulation, abnormal cholesterol profiles and metabolism, oxidative stress, reduced endothelium integrity, vascular reactivity, and reduced cerebral blood flow [9]. In an earlier clinical trial, we have shown that WM microstructure, even in the most vulnerable prefrontal regions, is malleable by aerobic exercise such as walking and dance [68,69]. Therefore, our results encourage future clinical trials that would assess the effects of reducing adiposity – in particular, visceral adiposity – on myelin integrity, to establish casual relationships between adiposity and myelin and to test the potential of weight reduction as a means for protecting the aging WM.

#### 4.3. Sex differences in MWF

Previous reports on sex differences in myelin content have been inconsistent. For example, using BMC-mcDESPOT to estimate myelin in 106 adults of age 22–94, Bouhrara et al., [70] found trend effects of sex, suggesting 10% higher myelin in women as compared to men in the parietal lobe and the body and the splenium of corpus callosum. Conversely, a study in 801 healthy participants of age 7–84 using R1 relaxation, sensitive to myelin, reported a trend for higher myelin content in SLF and arcuate fasciculus in men as compared to women [52]. Regarding interactions of age and sex, both studies reported trend results, suggesting marginally greater reduction in myelin with age in women as compared to men (in the thalamic radiations, cingulum, SLF, arcuate and inferior fronto-occipital fasciculus bundle according to [52], and in whole WM, temporal lobes, the body of corpus callosum the anterior and the posterior corona radiata according to [62]). Therefore, our results of no significant sex or sex\*age effects on MWF neither confirm or infirm these earlier studies, but suggest that the effects of sex on myelin during adulthood may be, overall, marginal.

#### 4.4. Limitations

The main limitation of our study is the self-reported status of a history of dyslipidemia and hyperglycemia. Such measurement may not only be inaccurate, but provide only a binary classification, which does not allow for evaluation of the impact of a range of fasting blood glucose, cholesterol and triglyceride levels on myelin content. The use of self-reported data may have introduced bias, as some participants might

have over- or underreported their condition or might not have been aware of existing abnormalities in their blood lipids or sugar levels. However, we would expect that this would underestimate rather than overestimate the MetS-myelin associations, namely, that our findings would have greater effects sizes if blood results were available. This may also explain that in-lab measures (i.e., BP, BMI, WC) showed consistent associations with MWF, whereas self-reported MetS components (blood lipid and glucose) did not.

Another possible limitation is that MWF values were affected by macrostructural changes related to age and MetS individual components, such as global brain tissue atrophy, presence of infarcts, silent strokes, and WM hyperintensities [9,10]. Importantly, we minimized the impact of cerebrovascular abnormalities on WM microstructure by strict inclusion and exclusion criteria, which was, indeed, the main reason for excluding middle-aged to older participants (Appendix A). As a result, our participants had at most only few punctuate deep WM hyperintensities. Second, we used TBSS to align and skeletonize MWF values in the center of WM tracts. This procedure has been shown to minimize the impact of age-related atrophy on the extracted values, and also excluded regions of lower FA such as affected by WMH. This means, the analysis was performed on the “best looking” voxels. Therefore, we speculate that the effects of MetS, its components, and age are underestimated rather than overestimated in our study. Also, using TBSS was aimed to minimize the effect of different voxel dimensions in acquisition of MWF maps and DTI maps (4 mm vs 1.8 mm slice thickness, respectively), although we acknowledge that some partial volume effects are unavoidable, even when using non-linear registrations.

Finally, our sample size was not large and we performed multiple inferential tests, which poses a risk of Type 1 error. However, it is important to note that this study is already a replication and extension of an earlier study [15], suggesting that the observed effects are unlikely to be false positives. Also, we refrained from focusing on the *p* values, even if FDR-corrected, and focused our interpretations on the effect sizes [71]. The ultimate test for our findings will be another replication in an independent sample.

#### 4.5. Conclusions

We have shown that MetS or pre-MetS are prevalent even in an above-average healthy adult sample, and that both MetS risk score and adiposity were related to lower myelin content, controlling for the effects of age, sex, race, ethnicity and socioeconomic factors. Our findings call for clinical trials that would assess the potential of weight loss and visceral adiposity reduction as means to support maintenance of myelin integrity throughout the adulthood. We argue that such studies would be especially needed in young to middle-aged adults, given the protracted myelination in the regions affected by adiposity. Namely, MetS- and adiposity-related processes could interfere with achieving peak myelin content and integrity in midlife, which could then predispose for accelerated brain aging and risk of Alzheimer’s disease. Importantly, decline in cerebral metabolic rate is one of the earliest indicators of Alzheimer’s disease risk [72], and failure of axonal transport and myelin repair is increasingly considered as early mechanisms of Alzheimer’s disease pathophysiology [11,59,65]. Thus, our findings urge identification of mechanisms linking MetS components with WM integrity at molecular and physiological levels, which could open new avenues for prevention and treatment of cognitive decline and dementia.

#### Declaration of Competing Interest

None.

#### Data availability

The data used to generate the results presented in this work is available upon request from the corresponding author, due to the

ongoing data collection.

## Acknowledgments

The study was supported by AARG-NTF-21-849265 from the Alzheimer's Association and 1R21AG068939-01A1 from the National Institutes on Aging to AZ Burzynska.

We thank the current and past members of the BRAiN lab for their help in data collection: Jake Lonergan, Raghuram Kakinada, Neveah Newton, Miles Hopkins, Nick Stirbis, Brandon Paez, and Tess Armstrong. We thank Vineet Agarwal for being the study data wizard. We thank all of your participants who volunteered for the study and Kelly Lyell for help with recruitment. We thank Joon Yul Choi for his help in GRASE image processing.

## Supplementary materials

Supplementary material associated with this article can be found, in the online version, at [doi:10.1016/j.cccb.2023.100180](https://doi.org/10.1016/j.cccb.2023.100180).

## References

- K.G.M.M. Alberti, P. Zimmet, J. Shaw, Metabolic syndrome - a new world-wide definition. A consensus statement from the International Diabetes Federation, *Diabetic Medicine* 23 (5) (2006), <https://doi.org/10.1111/j.1464-5491.2006.01858.x>.
- R. Chen, S. Safiri, M. Behzadifar, J.D. Kong, M.S. Zguira, N.L. Bragazzi, W. Zhong, W. Zhang, Health effects of metabolic risks in the United States from 1990 to 2019, *Front. Public Health* 10 (2022), <https://doi.org/10.3389/fpubh.2022.751126>.
- G. Razay, A. Vreugdenhil, G. Wilcock, The metabolic syndrome and Alzheimer disease, *Arch. Neurol.* 64 (1) (2007), <https://doi.org/10.1001/archneur.64.1.93>.
- K. Yaffe, A. Kanaya, K. Lindquist, E.M. Simonsick, T. Harris, R.I. Shorr, F. A. Tylavsky, A.B. Newman, The metabolic syndrome, inflammation, and risk of cognitive decline, *JAMA* (18) (2004) 292, <https://doi.org/10.1001/jama.292.18.2237>.
- R.B. Ervin, Prevalence of metabolic syndrome among adults 20 years of age and over, by sex, age, race and ethnicity, and body mass index: united States, 2003-2006, *Natl. Health Stat. Rep.* (2009) 13.
- H.M. Lakka, D.E. Laaksonen, T.A. Lakka, L.K. Niskanen, E. Kumpusalo, J. Tuomilehto, J.T. Salonen, The metabolic syndrome and total and cardiovascular disease mortality in middle-aged men, *J. Am. Med. Assoc.* (21) (2002) 288, <https://doi.org/10.1001/jama.288.21.2709>.
- Q. Yin, X. Chen, L. Li, R. Zhou, J. Huang, D. Yang, Apolipoprotein B/apolipoprotein A1 ratio is a good predictive marker of metabolic syndrome and pre-metabolic syndrome in Chinese adolescent women with polycystic ovary syndrome, *J. Obstetr. Gynaecol. Res.* (1) (2013) 39, <https://doi.org/10.1111/j.1447-0756.2012.01907.x>.
- World Health Organization. (2021). *Obesity and overweight*. <https://www.who.int/news-room/fact-sheets/detail/obesity-and-overweight>.
- F.J. Alfaro, A. Gavrieli, P. Saade-Lemus, V.A. Lioutas, J. Upadhyay, V. Novak, White matter microstructure and cognitive decline in metabolic syndrome: a review of diffusion tensor imaging, *Metab. Clin. Exp.* 78 (2018), <https://doi.org/10.1016/j.metabol.2017.08.009>.
- K.F. Yates, V. Sweat, P.L. Yau, M.M. Turchiano, A. Convit, Impact of Metabolic Syndrome on Cognition and Brain, *Arterioscler. Thromb. Vasc. Biol.* (9) (2012) 32, <https://doi.org/10.1161/atvbaha.112.252759>.
- G. Bartzokis, Age-related myelin breakdown: a developmental model of cognitive decline and Alzheimer's disease, *Neurobiol. Aging* 25 (1) (2004) 5-18. <http://www.ncbi.nlm.nih.gov/pubmed/14675724>.
- B. Polis, A.O. Samson, A new perspective on Alzheimer's disease as a brain expression of a complex metabolic disorder, in: T. Wisniewski (Ed.), *Alzheimer's Disease*, Codon Publications, Brisbane (AU), 2019, <https://doi.org/10.15586/alzheimersdisease.2019.ch1>.
- D.K. Jones, M. Cercignani, Twenty-five pitfalls in the analysis of diffusion MRI data, *NMR Biomed.* 23 (7) (2010) 803-820, <https://doi.org/10.1002/nbm.1543>.
- J. Lee, J.W. Hyun, J. Lee, E.J. Choi, H.G. Shin, K. Min, Y. Nam, H.J. Kim, S.H. Oh, So you want to image myelin using MRI: an overview and practical guide for myelin water imaging, *J. Magnet. Reson. Imag.* 53 (2) (2020) 360-373, <https://doi.org/10.1002/jmri.27059>.
- M. Bouhrara, N. Khattar, P. Elango, S.M. Resnick, L. Ferrucci, R.G. Spencer, Evidence of association between obesity and lower cerebral myelin content in cognitively unimpaired adults, *Int. J. Obes.* (4) (2021) 45, <https://doi.org/10.1038/s41366-021-00749-x>.
- K. Mueller, A. Anwander, H.E. Möller, A. Horstmann, J. Lepsien, F. Busse, S. Mohammadi, M.L. Schroeter, M. Stumvoll, A. Villringer, B. Pleger, Sex-dependent influences of obesity on cerebral white matter investigated by diffusion-tensor imaging, *PLoS ONE* 6 (4) (2011), <https://doi.org/10.1371/journal.pone.0018544>.
- K.M. Stanek, S.M. Grieve, A.M. Brickman, M.S. Korgaonkar, R.H. Paul, R.A. Cohen, J.J. Gunstad, Obesity is associated with reduced white matter integrity in otherwise healthy adults, *Obesity* (3) (2011) 19, <https://doi.org/10.1038/oby.2010.312>.
- T.D. Verstynen, A.M. Weinstein, W.W. Schneider, J.M. Jakicic, D.L. Rofey, K. I. Erickson, Increased body mass index is associated with a global and distributed decrease in white matter microstructural integrity, *Psychosom. Med.* (7) (2012) 74, <https://doi.org/10.1097/PSY.0b013e318261909c>.
- T.D. Verstynen, A. Weinstein, K.I. Erickson, L.K. Sheu, A.L. Marsland, P. J. Gianaros, Competing physiological pathways link individual differences in weight and abdominal adiposity to white matter microstructure, *Neuroimage* 79 (2013), <https://doi.org/10.1016/j.neuroimage.2013.04.075>.
- J. Xu, Y. Li, H. Lin, R. Sinha, M.N. Potenza, Body mass index correlates negatively with white matter integrity in the fornix and corpus callosum: a diffusion tensor imaging study, *Hum. Brain Mapp.* (5) (2013) 34, <https://doi.org/10.1002/hbm.21491>.
- G. Bartzokis, D. Sultzer, P.H. Lu, K.H. Nuechterlein, J. Mintz, J.L. Cummings, Heterogeneous age-related breakdown of white matter structural integrity: implications for cortical "disconnection" in aging and Alzheimer's disease, *Neurobiol. Aging* 25 (7) (2004) 843-851, <https://doi.org/10.1016/j.neurobiolaging.2003.09.005>.
- L. Marnier, J.R. Nyengaard, Y. Tang, B. Pakkenberg, Marked loss of myelinated nerve fibers in the human brain with age, *J. Comparat. Neurol.* 462 (2) (2003) 144-152, <https://doi.org/10.1002/cne.10714>.
- E. Etchells, G. Sharpe, C. Elliott, A. Singer, *CMAJ* 155 (6) (1996) 657-661.
- S.Y. Bookheimer, D.H. Salat, M. Terpsstra, B.M. Ances, D.M. Barch, R.L. Buckner, G. C. Burgess, S.W. Curtiss, M. Diaz-Santos, J.S. Elam, B. Fischl, D.N. Greve, H. A. Hagy, M.P. Harms, O.M. Hatch, T. Hedden, C. Hodge, K.C. Japardi, T.P. Kuhn, E. Yacoub, The lifespan human connectome project in aging: an overview, *Neuroimage* 185 (2019) 335-348, <https://doi.org/10.1016/j.neuroimage.2018.10.009>.
- C.A. de Jager, M.M. Budge, R. Clarke, Utility of TIGS-M for the assessment of cognitive function in older adults, *Int. J. Geriatr. Psychiatry* 18 (4) (2003) 318-324, <https://doi.org/10.1002/gps.830>.
- B.W. Rovner, M.F. Folstein, Mini-mental state exam in clinical practice, *Hosp. Pract. (Off. Ed.)* 22 (1A) (1987) 99. <http://www.ncbi.nlm.nih.gov/pubmed/3100557>.
- R.M. Crum, J.C. Anthony, S.S. Bassett, M.F. Folstein, Population-based norms for the mini-mental state examination by age and educational level, *JAMA: J. Am. Med. Assoc.* 269 (18) (1993) 2386-2391, <https://doi.org/10.1001/jama.1993.03500180078038>.
- J.C. Morris, The clinical dementia rating (CDR): current version and scoring rules, *Neurology* 43 (1993) 2412, <https://doi.org/10.1212/wnl.43.11.2412-a>.
- J.A. Yasavage, J.I. Sheikh, Geriatric depression scale (GDS): recent evidence and development of a shorter version, *Clin. Gerontol.* 5 (1-2) (1986) 165-173.
- I.M. Nasrallah, N.M. Pajewski, A.P. Auchus, G. Chelune, A.K. Cheung, M. L. Cleveland, L.H. Coker, M.G. Crowe, W.C. Cushman, J.A. Cutler, C. Davatzikos, L. Desiderio, J. Doshi, G. Erus, L.J. Fine, S.A. Gaussoin, D. Harris, K.C. Johnson, P. L. Kimmel, R.N. Bryan, Association of intensive vs standard blood pressure control with cerebral white matter lesions, *JAMA - J. Am. Med. Assoc.* 322 (6) (2019) 524-534, <https://doi.org/10.1001/jama.2019.10551>.
- N. Medic, P. Kochunov, H. Ziauddeen, K.D. Ersche, P.J. Nathan, L. Ronan, P. C. Fletcher, BMI-related cortical morphometry changes are associated with altered white matter structure, *Int. J. Obes.* 43 (3) (2019) 1, <https://doi.org/10.1038/s41366-018-0269-9>.
- J.E. Winter, R.J. MacLinnis, N. Wattanapenpaiboon, C.A. Nowson, BMI and all-cause mortality in older adults: a meta-analysis, *Am. J. Clin. Nutr.* 99 (4) (2014) 875-890, <https://doi.org/10.3945/ajcn.113.068122>.
- W.G. Rosen, R.D. Terry, P.A. Fuld, R. Katzman, A. Peck, Pathological verification of ischemic score in differentiation of dementias, *Ann. Neurol.* 7 (5) (1980) 486-488, <https://doi.org/10.1002/ana.410070516>.
- T.A. Salthouse, Decomposing age correlations on neuropsychological and cognitive variables, *J. Int. Neuropsychol. Soc.* : JINS 15 (5) (2009) 650-661, <https://doi.org/10.1017/S1355617709990385>.
- R.K. Heaton, N. Akshoomoff, D. Tulsky, D. Mungas, S. Weintraub, S. Dikmen, J. Beaumont, K.B. Casaletto, K. Conway, J. Slotkin, R. Gershon, Reliability and validity of composite scores from the NIH toolbox cognition battery in adults, *J. Int. Neuropsychol. Soc.* 20 (6) (2014) 588-598, <https://doi.org/10.1017/S1355617714000241>.
- S. Weintraub, S.S. Dikmen, R.K. Heaton, D.S. Tulsky, P.D. Zelazo, P.J. Bauer, N. E. Carlozzi, J. Slotkin, D. Blitz, K. Wallner-Allen, N.A. Fox, J.L. Beaumont, D. Mungas, C.J. Nowinski, J. Richler, J.A. Deocampo, J.E. Anderson, J.J. Manly, B. Borosh, R.C. Gershon, Cognition assessment using the NIH Toolbox, *Neurology* 80 (11 Suppl 3) (2013) S54-S64, <https://doi.org/10.1212/wnl.0b013e3182872ded>.
- T. Prasloski, A. Rauscher, A.L. MacKay, M. Hodgson, I.M. Vavasour, C. Laule, B. Mädler, Rapid whole cerebrum myelin water imaging using a 3D GRASE sequence, *Neuroimage* (1) (2012) 63, <https://doi.org/10.1016/j.neuroimage.2012.06.064>.
- J.L.R. Andersson, S. Skare, J. Ashburner, How to correct susceptibility distortions in spin-echo echo-planar images: application to diffusion tensor imaging, *Neuroimage* 20 (2) (2003) 870-888, [https://doi.org/10.1016/S1053-8119\(03\)00336-7](https://doi.org/10.1016/S1053-8119(03)00336-7).
- S.M. Smith, M. Jenkinson, M.W. Woolrich, C.F. Beckmann, T.E.J. Behrens, H. Johansen-Berg, P.R. Bannister, M. De Luca, I. Drobnjak, D.E. Flitney, R.K. Niazy, J. Saunders, J. Vickers, Y. Zhang, N. De Stefano, J.M. Brady, P.M. Matthews,

- Advances in functional and structural MR image analysis and implementation as FSL, *Neuroimage* 23 (1) (2004) S208–S219, <https://doi.org/10.1016/j.neuroimage.2004.07.051>.
- [40] J.L.R. Andersson, S.N. Sotiropoulos, An integrated approach to correction for off-resonance effects and subject movement in diffusion MR imaging, *Neuroimage* 125 (2016), <https://doi.org/10.1016/j.neuroimage.2015.10.019>.
- [41] S.M. Smith, H. Johansen-Berg, M. Jenkinson, D. Rueckert, T.E. Nichols, K.L. Miller, M.D. Robson, D.K. Jones, J.C. Klein, A.J. Bartsch, T.E.J. Behrens, Acquisition and voxelwise analysis of multi-subject diffusion data with tract-based spatial statistics, *Nat. Protoc.* 2 (3) (2007) 499–503. <http://www.ncbi.nlm.nih.gov/pubmed/17406613>.
- [42] D. Rueckert, L.I. Sonoda, C. Hayes, D.L. Hill, M.O. Leach, D.J. Hawkes, Nonrigid registration using free-form deformations: application to breast MR images, *IEEE Trans. Med. Imag.* 18 (8) (1999) 712–721, <https://doi.org/10.1109/42.796284>.
- [43] A.Z. Burzynska, D.D. Garrett, C. Preuschhof, I.E. Nagel, S.-C. Li, L. Bäckman, H. R. Heekeren, U. Lindenberger, A scaffold for efficiency in the human brain, *J. Neurosci. : Off. J. Soc. Neurosci.* 33 (43) (2013) 17150–17159, <https://doi.org/10.1523/JNEUROSCI.1426-13.2013>.
- [44] S. Mori, S. Wakana, L.M. Nagae-Poetscher, P.C. van Zijl, *MRI Atlas of Human White Matter (First)*, Elsevier, 2005.
- [45] S. Hofer, J. Frahm, Topography of the human corpus callosum revisited—comprehensive fiber tractography using diffusion tensor magnetic resonance imaging, *Neuroimage* 32 (3) (2006) 989–994, <https://doi.org/10.1016/j.neuroimage.2006.05.044>.
- [46] P. Muntner, D. Shimbo, R.M. Carey, J.B. Charleston, T. Gaillard, S. Misra, M. G. Myers, G. Ogedegbe, J.E. Schwartz, R.R. Townsend, E.M. Urbina, A.J. Viera, W. B. White, J.T. Wright, Measurement of blood pressure in humans: a scientific statement from the American Heart Association, *Hypertension* (5) (2019) 73, <https://doi.org/10.1161/HYP.000000000000087>.
- [47] World Health Organization. (1995). *Physical status: the use of and interpretation of anthropometry, Report of a WHO Expert Committee*. <https://apps.who.int/iris/handle/10665/37003>.
- [48] World Health Organization. (2011). *Waist Circumference and Waist-to-Hip Ratio: a Report of a WHO expert consultation*. WHO Nutrition and Food Safety team. <http://www.who.int/publications/i/item/9789241501491>.
- [49] G.M.A.I. Kibria, R. Crispen, M.A.B. Chowdhury, N. Rao, C. Stennett, Disparities in absolute cardiovascular risk, metabolic syndrome, hypertension, and other risk factors by income within racial/ethnic groups among middle-aged and older US people, *J. Hum. Hypertens.* (2021), <https://doi.org/10.1038/s41371-021-00513-8>.
- [50] E.B. Loucks, D.H. Rehkopf, R.C. Thurston, I. Kawachi, Socioeconomic disparities in metabolic syndrome differ by gender: evidence from NHANES III, *Ann. Epidemiol.* 17 (1) (2007), <https://doi.org/10.1016/j.annepidem.2006.07.002>.
- [51] M. Bouhrara, D.A. Reiter, C.M. Bergeron, L.M. Zukley, L. Ferrucci, S.M. Resnick, R. G. Spencer, Evidence of demyelination in mild cognitive impairment and dementia using a direct and specific magnetic resonance imaging measure of myelin content, *Alzheimer. Dement.* 14 (8) (2018) 998–1004, <https://doi.org/10.1016/j.jalz.2018.03.007>.
- [52] D.A. Slater, L. Melie-Garcia, M. Preisig, F. Kherif, A. Lutti, B. Draganski, Evolution of white matter tract microstructure across the life span, *Hum. Brain Mapp.* 40 (7) (2019) 2252–2268, <https://doi.org/10.1002/hbm.24522>.
- [53] T. Billiet, M. Vandenbulcke, B. Mädlar, R. Peeters, T. Dhollander, H. Zhang, S. Deprez, B.R.H. Van den Bergh, S. Sunaert, L. Emsell, Age-related microstructural differences quantified using myelin water imaging and advanced diffusion MRI, *Neurobiol. Aging* 36 (6) (2015) 2107–2121, <https://doi.org/10.1016/j.neurobiolaging.2015.02.029>.
- [54] T.D. Faizy, D. Kumar, G. Broocks, C. Thaler, F. Flottmann, H. Leischner, D. Kutzner, S. Hewera, D. Dotzauer, J.P. Stellmann, R. Reddy, J. Fiehler, J. Sedlaciak, S. Gellißen, Age-related measurements of the myelin water fraction derived from 3D multi-echo GRASE reflect myelin content of the cerebral white matter, *Sci. Rep.* 8 (1) (2018), <https://doi.org/10.1038/s41598-018-33112-8>.
- [55] A.R. Bender, N. Raz, Normal-appearing cerebral white matter in healthy adults: mean change over 2 years and individual differences in change, *Neurobiol. Aging* (5) (2015) 36, <https://doi.org/10.1016/j.neurobiolaging.2015.02.001>.
- [56] H.C. Kinney, J.J. Volpe, Myelination Events. Volpe's Neurology of the Newborn, Elsevier, 2018, pp. 176–188, <https://doi.org/10.1016/B978-0-323-42876-7.00008-9>.
- [57] J.D. Lynn, C. Anand, M. Arshad, R. Homayouni, D.R. Rosenberg, N. Ofen, N. Raz, J. A. Stanley, Microstructure of human corpus callosum across the lifespan: regional variations in axon caliber, density, and myelin content, *Cerebral. Cortex* (2) (2021) 31, <https://doi.org/10.1093/cercor/bhaa272>.
- [58] Armati, P.J., & Mathey, E.K. (Eds). (2010). *The Biology of Oligodendrocytes*. <https://doi.org/10.1017/CBO9780511782121>.
- [59] G. Bartzokis, Alzheimer's disease as homeostatic responses to age-related myelin breakdown, *Neurobiol. Aging* 32 (2011) 1341–1371, <https://doi.org/10.1016/j.neurobiolaging.2009.08.007>.
- [60] F. Aboitiz, A.B. Scheibel, R.S. Fisher, E. Zaidel, Fiber composition of the human corpus callosum, *Brain Res.* 598 (1–2) (1992) 143–153. <http://www.ncbi.nlm.nih.gov/pubmed/1486477>.
- [61] A.C. Birdsill, C.M. Carlsson, A.A. Willette, O.C. Okonkwo, S.C. Johnson, G. Xu, J. M. Oh, C.L. Gallagher, R.L. Kosciak, E.M. Jonaitis, B.P. Hermann, A. LaRue, H. A. Rowley, S. Asthana, M.A. Sager, B.B. Bendlin, Low cerebral blood flow is associated with lower memory function in metabolic syndrome, *Obesity (Silver Spring)* 21 (7) (2013) 1313–1320, <https://doi.org/10.1002/oby.20170>.
- [62] M. Bouhrara, A.C. Rejimon, L.E. Cortina, N. Khattar, C.M. Bergeron, L. Ferrucci, S. M. Resnick, R.G. Spencer, Adult brain aging investigated using BMC-mcDESPOT-based myelin water fraction imaging, *Neurobiol. Aging* 85 (2020) 131–139, <https://doi.org/10.1016/j.neurobiolaging.2019.10.003>.
- [63] M. Simons, K.A. Nave, Oligodendrocytes: myelination and axonal support, *Cold Spring Harb. Perspect. Biol.* 8 (1) (2016) 020479, <https://doi.org/10.1101/cshperspect.a020479>.
- [64] K.A. Nave, Myelination and the trophic support of long axons, *Nat. Rev. Neurosci.* 11 (4) (2010), <https://doi.org/10.1038/nrn2797>.
- [65] S.E. Nasrabady, B. Rizvi, J.E. Goldman, A.M. Brickman, White matter changes in Alzheimer's disease: a focus on myelin and oligodendrocytes, *Acta Neuropathol. Commun.* 6 (1) (2018) 22, <https://doi.org/10.1186/s40478-018-0515-3>.
- [66] M.C. Power, J.V. Tingle, R.I. Reid, J. Huang, A.R. Sharrett, J. Coresh, M. Griswold, K. Kantarci, C.R. Jack, D. Knopman, R.F. Gottesman, T.H. Mosley, Midlife and late-life vascular risk factors and white matter microstructural integrity: the atherosclerosis risk in communities neurocognitive study, *J. Am. Heart Assoc.* 6 (5) (2017), <https://doi.org/10.1161/JAHA.117.005608>.
- [67] M. Sala, A. De Roos, A. Van Den Berg, I. Altmann-Schneider, P. Eline Slagboom, R. G. Westendorp, M.A. Van Buchem, A.J.M. De Craen, J. Van Der Grond, Microstructural brain tissue damage in metabolic syndrome, *Diabet. Care* (2) (2014) 37, <https://doi.org/10.2337/dci13-1160>.
- [68] A.Z. Burzynska, Y. Jiao, A.M. Knecht, J. Fanning, E.A. Awick, T. Chen, N. Gothe, M. W. Voss, E. McAuley, A.F. Kramer, White matter integrity declined over 6-months, but dance intervention improved integrity of the Fornix of older adults, *Front. Aging Neurosci.* 9 (2017) 59, <https://doi.org/10.3389/fnagi.2017.00059>.
- [69] A. Mendez Colmenares, M.W. Voss, J. Fanning, E.A. Salerno, N.P. Gothe, M. L. Thomas, E. McAuley, A.F. Kramer, A.Z. Burzynska, White matter plasticity in healthy older adults: the effects of aerobic exercise, *Neuroimage* 239 (2021), 118305, <https://doi.org/10.1016/j.neuroimage.2021.118305>.
- [70] M. Bouhrara, J.S.R. Alisch, N. Khattar, et al., Association of cerebral blood flow with myelin content in cognitively unimpaired adults, *BMJ Neurol. Open* 2 (2020), e000053, <https://doi.org/10.1136/bmjno-2020-000053>.
- [71] G.M. Sullivan, R. Feinn, Using effect size-or why the P value is not enough, *J. Grad. Med. Educ.* 4 (3) (2012) 279–282, <https://doi.org/10.4300/JGME-D-12-00156.1>.
- [72] M. Pagani, F. Nobili, S. Morbelli, D. Arnaldi, A. Giuliani, J. Öberg, N. Girtler, A. Brugnolo, A. Picco, M. Bauckneht, R. Piva, A. Chincarini, G. Sambucetti, C. Jonsson, F. De Carli, Early identification of MCI converting to AD: a FDG PET study, *Eur. J. Nucl. Med. Mol. Imaging* (12) (2017) 44, <https://doi.org/10.1007/s00259-017-3761-x>.